

DEM-Simulation of thin elastic membranes interacting with a granulate

Holger Götz · Thorsten Pöschel

Received: October 20, 2022/ Accepted: date

Abstract For a wide range of applications, we need DEM simulations of granular matter in contact with elastic flexible boundaries. We present a novel method to describe the interaction between granular particles and a flexible elastic membrane. Here, the standard mass-spring model approach is supplemented by surface patches given by a triangulation of the membrane. In contrast to standard mass-spring models, our simulation method allows for an efficient simulation even for large particle size dispersion. The novel method allows coarsening of the mass-spring system leading to a substantial increase of computation efficiency. The simulation method is demonstrated and benchmarked for a triaxial test.

Keywords DEM · boundary condition · elastic membrane · triaxial test

1 Introduction

For many applications in granular matter research, the system boundaries are given by deformable containers which may be modeled as elastic membranes. Of particular interest are jamming systems where the granulate changes its mechanical properties drastically when the particle number density in the system is changed [1, 2, 3], which is frequently achieved by evacuating the air from a deformable container partly filled by granulate. Prominent examples are granular robotic grippers [4],

where this mechanism is used to grip and manipulate objects, granular paws [5] and similar [6].

In these cases, the system dynamics is determined by two-way coupling, that is, the deformation of the membrane (e.g. caused by external air pressure) implies forces on the granular particles and the membrane is deformed under the action of the granular packing. Such membranes can be modeled as *mass-spring systems* (MSS), e.g. [7]. Here the membrane is described as a regular or irregular graph whose vertices are particles and whose edges are linear or non-linear elastic springs. The elastic behavior is, thus, described by the springs and the contacts between the membrane and the enclosed granular particles are described by the contacts between the membrane's particles and the particles of the granulate.

The choice of the membrane's structure is critical: If the meshes are too coarse, particles can penetrate the membrane. Therefore, the mesh width has to be chosen according to the smallest particles in the system [8, 7]. This is problematic for several reasons: First, in the course of the simulation when the membrane and the granulate particles interact, the mesh width may change which is difficult to predict. Second, for the simulation of a highly disperse granulate, the number of membrane particles and springs can be very large, resulting in an inefficient simulation. The problem can be solved by artificially increasing the sizes of the non-interacting membrane particles (overlapping particles) [9] which, however, introduces an undesired thickness of the membrane. All MSS models are problematic for the modeling of tangential (frictional) forces along the membrane since the contacts of the membrane particles - granular particles depends on the concrete arrangement of the particle positions.

Holger Götz · Thorsten Pöschel
Institute for Multiscale Simulations
Friedrich-Alexander-Universität Erlangen-Nürnberg
Cauerstraße 3, 91058 Erlangen
Germany
E-mail: holger.goetz@fau.de

In the current paper, we describe a novel type of MSS which allows for the simulation of impenetrable flexible elastic boundaries requiring a moderate number of membrane particles. This model does not suffer from the drawbacks discussed above. Since by construction the membrane is impenetrable, the meshes can be chosen larger which makes our method computationally efficient. The proposed model was used recently to simulate a granular gripper [10] and a bending beam of granular meta-material [11].

2 Model description

2.1 Particle: particle interaction

The discrete element method (DEM) solves Newton's equation for the position \mathbf{r}_i and the angular orientation φ_i of each particle, i , of mass m_i and tensorial moment of inertia, \hat{J}_i :

$$m_i \frac{d^2 \mathbf{r}_i}{dt^2} = \mathbf{F}_i = \sum_{j \neq i} \mathbf{F}_{ij} + \mathbf{F}_i^{\text{ext}}, \quad (1)$$

$$\hat{J}_i \frac{d^2 \varphi_i}{dt^2} = \mathbf{M}_i = \sum_{j \neq i} \mathbf{M}_{ij}. \quad (2)$$

Here, $\mathbf{F}_i^{\text{ext}}$ is an external force, e.g. gravity, and \mathbf{F}_{ij} and \mathbf{M}_{ij} are the force and torque acting on particle i due to contacts with particles j . There are several models for \mathbf{F}_{ij} and \mathbf{M}_{ij} as functions of the relative position, orientation, velocity and angular velocity of the involved particles, i and j , for an extended discussion see, e.g., [12, 13, 14, 15, 16].

2.2 Membrane: topology

In the current paper, we focus on the description of an ambient membrane and its interaction with the granular particles. In our model, the elastically deformable membrane is modeled by mass-carrying particles that are connected by viscoelastic springs (mass-spring system, MSS). The topology of the membrane is given by a mathematical graph whose vertices and edges are represented by particles and springs, respectively.

The positions of the membrane particles (here called vertex particles), thus, describe the shape of the membrane (Fig. 1). They are subject of Newton's equations where the forces acting on the vertex membrane particles originate from three contributions: (a) viscoelastic stretching of the membrane, (b) moments due to bending of the membrane, and (c) interaction of granular particles with the membrane. We shall discuss these

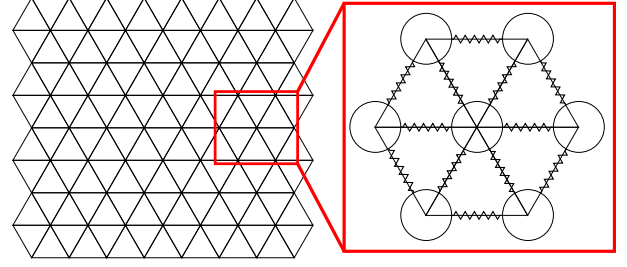


Fig. 1 Sketch of the MSS

contributions in Secs. 2.3-2.5. The total force acting on the vertex particles is the sum of these three contributions.

2.3 Membrane: stretching

Given two adjacent vertex particles i, j at positions $\boldsymbol{\rho}_i, \boldsymbol{\rho}_j$ and velocities $\dot{\boldsymbol{\rho}}_i, \dot{\boldsymbol{\rho}}_j$, we define the relative quantities

$$\boldsymbol{\rho}_{ij} \equiv \boldsymbol{\rho}_i - \boldsymbol{\rho}_j, \quad (3)$$

$$\dot{\boldsymbol{\rho}}_{ij} \equiv \dot{\boldsymbol{\rho}}_i - \dot{\boldsymbol{\rho}}_j \quad (4)$$

and the unit vector

$$\hat{\boldsymbol{\rho}}_{ij} \equiv \frac{\boldsymbol{\rho}_{ij}}{\rho_{ij}}. \quad (5)$$

The interaction between particles i and j is due to linear elastic spring. Particle i feels the force

$$\mathbf{F}_{ij}^{\text{spring}} = \hat{\boldsymbol{\rho}}_{ij} \left[k (\rho_{ij} - \rho_{ij}^0) - 2\gamma \sqrt{k m_{ij}^{\text{eff}}} \hat{\boldsymbol{\rho}}_{ij} \cdot \dot{\boldsymbol{\rho}}_{ij} \right], \quad (6)$$

which is the force of a damped harmonic oscillator, with equilibrium length ρ_{ij}^0 , effective mass $m_{ij}^{\text{eff}} = m_i m_j / (m_i + m_j)$, damping coefficient γ , and spring constant k .

To relate the spring constant, k , to material characteristics, we notice that each realistic membrane has a finite width, d , and the elasticity of the membrane material is characterized by its elastic modulus E . For our idealized two-dimensional membrane of vanishing thickness, one obtains the elastic constant [17, 18].

$$k = \frac{\sqrt{3}}{2} E d. \quad (7)$$

2.4 Membrane: flexibility

To explain the description of membrane flexibility, we consider four adjacent vertex particles at positions $\boldsymbol{\rho}_1, \boldsymbol{\rho}_2, \boldsymbol{\rho}_3, \boldsymbol{\rho}_4$ [19], see Fig. 2. The vertex particles span two triangles with normal vectors

$$\mathbf{n}_1 = (\boldsymbol{\rho}_1 - \boldsymbol{\rho}_3) \times (\boldsymbol{\rho}_1 - \boldsymbol{\rho}_4) \quad (8)$$

$$\mathbf{n}_2 = (\boldsymbol{\rho}_2 - \boldsymbol{\rho}_4) \times (\boldsymbol{\rho}_2 - \boldsymbol{\rho}_3). \quad (9)$$

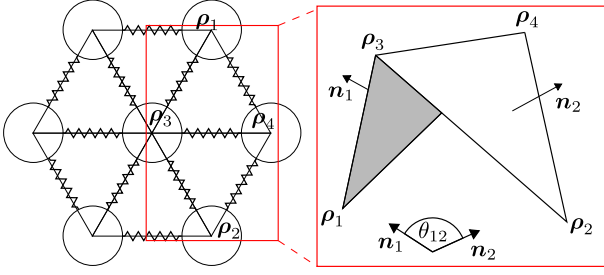


Fig. 2 The deformation of the membrane is described by the angle θ_{12} between the normal vectors of adjacent triangles $\triangle 134$ and $\triangle 243$. θ_{12} is extremely exaggerated in this sketch.

The corresponding angle θ_{12}

$$\cos \theta_{12} \equiv \mathbf{n}_1 \cdot \mathbf{n}_2 \quad (10)$$

characterizes the flecion of the triangles, with respect to their common edge $\rho_{43} = \rho_4 - \rho_3$. The restoring torque counteracting the flecion can be expressed by elastic and dissipative forces, \mathbf{F}_i^{el} , acting on the involved vertex particles, $i \in \{1, 2, 3, 4\}$ [19],

$$\mathbf{F}_i^{\text{el}} = k^{\text{el}} \frac{|\rho_{43}|^2}{|\mathbf{n}_1| + |\mathbf{n}_2|} \left(\sin \frac{\theta_{12}}{2} - \sin \frac{\theta_{12}^0}{2} \right) \mathbf{u}_i, \quad (11)$$

$$\mathbf{F}_i^{\text{diss}} = -k^{\text{diss}} |\rho_{43}| \dot{\theta}_{12} \mathbf{u}_i, \quad (12)$$

where k^{el} and k^{diss} are material parameters.

The directions of the forces are linear combinations of the triangles' normal vectors given by

$$\mathbf{u}_1 = |\rho_{43}| \frac{\mathbf{n}_1}{|\mathbf{n}_1|^2}, \quad (13)$$

$$\mathbf{u}_2 = |\rho_{43}| \frac{\mathbf{n}_2}{|\mathbf{n}_2|^2}, \quad (14)$$

$$\mathbf{u}_3 = \frac{(\mathbf{x}_1 - \mathbf{x}_4) \cdot \rho_{43}}{|\rho_{43}|} \frac{\mathbf{n}_1}{|\mathbf{n}_1|^2} + \frac{(\mathbf{x}_2 - \mathbf{x}_4) \cdot \rho_{43}}{|\rho_{43}|} \frac{\mathbf{n}_2}{|\mathbf{n}_2|^2}, \quad (15)$$

$$\mathbf{u}_4 = \frac{(\mathbf{x}_1 - \mathbf{x}_3) \cdot \rho_{43}}{|\rho_{43}|} \frac{\mathbf{n}_1}{|\mathbf{n}_1|^2} + \frac{(\mathbf{x}_2 - \mathbf{x}_3) \cdot \rho_{43}}{|\rho_{43}|} \frac{\mathbf{n}_2}{|\mathbf{n}_2|^2}. \quad (16)$$

Each vertex particle is involved in 6 different pairs of triangles, see Fig. 1. The total force acting on a vertex particle is, thus, the sum of the 6 corresponding forces given by Eqs. (11, 12).

2.5 Membrane: granulate-membrane interaction

For the description of the interaction between the membrane and the confined granular particles, we assume triangular patches spanned between the time dependent momentary positions of adjacent vertex particles, Fig. 3. The interaction of the granular particles with the membrane is then described by contacts between

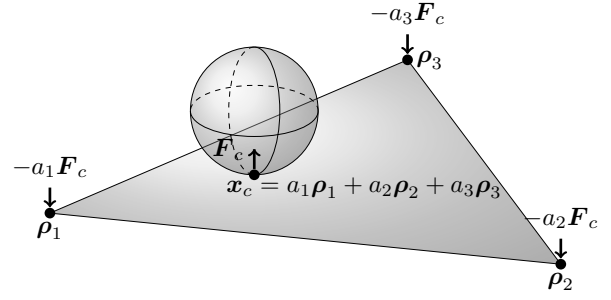


Fig. 3 Sketch of a contact between a granular particle and a triangular patch. The resulting force \mathbf{F}_c is mapped to the involved vertex particles ρ_1, ρ_2, ρ_3 according to the barycentric weights a_1, a_2, a_3 of the contact point \mathbf{x}_c with respect to the locations of the vertex particles.

the granular particles and the patches. This assures that the patches are always impenetrable disregarding of the sizes of the particles and the deformation of the membrane.

Contacts between a patch and a granular particle are classified as vertex, edge, or face contact:

vertex contact if $\mathbf{x}_c = \rho_i; i \in \{1, 2, 3\}$

edge contact if $(\mathbf{x}_c - \rho_j) \times (\rho_i - \rho_j) = \mathbf{0};$
 $i, j \in \{1, 2, 3\}; i \neq j$ (17)

face contact else

In case a granular particle contacts two neighboring patches, A and B , we chose the adequate contacts according to Tab. 1 in dependence whether these contacts are face, edge, or vertex contacts [20] These selection

	face A	edge A	vertex A
face B	A and B	B	B
edge B	A	A or B (rand)	B
vertex B	A	A	A or B (rand)

Table 1 Selection of contacts for the case that a granular particle ist in contact with two adjacent patches, A and B

rules do only apply if the patches A and B have a common edge. Otherwise, all contacts are handles regularly.

In case a granular particle contacts three neighboring patches at their common vertex, one of these contacts is selected randomly and the others are disregarded.

Contacts of the membrane with itself may be calculated from contacts between vertex particles and triangular patches.

Once the contact point is defined, we compute the force according to the specified contact law. The relative velocity of the granular particle and the membrane at the contact point which enters the force is interpolated from the velocities of the vertex particles using

barycentric weights, as sketched in Fig. 3. Similarly, the obtained force is distributed to the involved vertex particles with barycentric weights a_1, a_2, a_3 . The positions and velocities of the vertex particles and, thus, the dynamics of the membrane are obtained by numerical integration in the same way as the granular particles.

The above selection rule above in combination with the barycentric partition of the force leads to smooth and physically plausible forces acting on the vertex particles. [20]

3 Applications

We implemented the described flexible wall into the DEM program MercuryDPM [21]. Here we present two examples of its application.

3.1 Triaxial test

The triaxial test is commonly used to investigate the mechanical properties of a granular sample. To that aim, the sample is placed between two parallel platens and wrapped by a cylindrical membrane, see Fig. 4. A

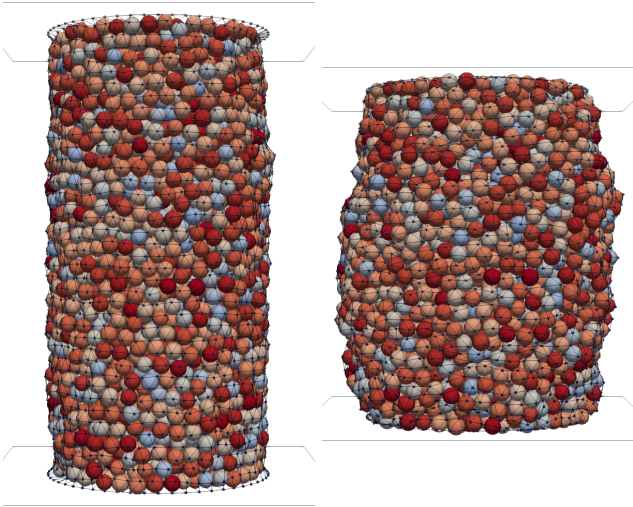


Fig. 4 A triaxial test cell in its initial and final states

confining stress σ_c in radial direction is applied through the membrane. By controlling the initial distance $h = h_0$ between the platens, an initial stress $\sigma_p = \sigma_c$ is applied in axial direction. Then, the platens are displaced at constant relative velocity \mathbf{v}_p to apply a strain $\epsilon = \log(h_0/h)$. We record the corresponding deviatoric stress $\sigma_d = \sigma_p - \sigma_c$.

In the simulation, we represent the platens by rigid walls and the membrane by an MSS. We place small

particles at random positions inside the membrane such that they do not contact one another. To generate the initial conditions, we apply the Lubachevsky–Stillinger algorithm [22]. We then gradually apply an initial stress, σ_p , to the platens and a confining stress, σ_c , to the membrane. To this end, each triangular patch of area A_i^w and normal unit vector $\hat{\mathbf{n}}_i^w$ is loaded with a force

$$\mathbf{F}_i^w = A_i^w \sigma_c \hat{\mathbf{n}}_i^w, \quad (18)$$

where $\hat{\mathbf{n}}_i^w$ is defined such that force acts from outside the membrane to the granulate located inside. After this initialization, we displace the platens at relative velocity \mathbf{v}_p and record the deviatoric stress, σ_d . Figure 4 shows the initial and final states of such a simulation.

To demonstrate the performance of our model, we perform simulations for two different cases:

1. We describe the membrane by a MSS where the confining stress of the membrane is provided by contacts between vertex particles and granular particles. This approach was used before, e.g., in [8]. We term this setup $MSS_{particle}$.
2. We describe the membrane as described in Sec. 2. Here the confining stress of the membrane is provided by contacts between the granular particles and the triangular patches. We term this setup MSS_{patch} .

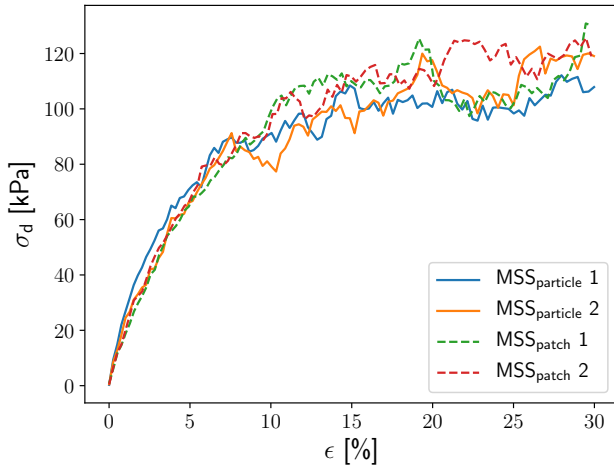
For $MSS_{particle}$, we place the vertex particles of the membrane spaced by $s = 1.33$ mm, such that the radius of a vertex particle is about 1/3 the radius of a granular particle. This value is a trade-off between keeping the computational cost low and having a smooth membrane that prevents penetration of granular particles [7, 8]. For MSS_{patch} , we use $s = 4.0$ mm because the membrane has a smooth surface and is impenetrable by design.

We perform the triaxial test at velocity $v_p = 0.05$ m/s and confining pressure $\sigma_c = 100$ kPa. The material parameters are given in Tab. 2. Furthermore, we choose the parameters $\gamma \approx 0.15$, $k^{\text{el}} = 10^{-3}$ N/m and $k^{\text{diss}} = 10^{-4}$ Ns/m. Using the initial areas of the triangles, we use Eqs. (11-16) to compute the confining forces.

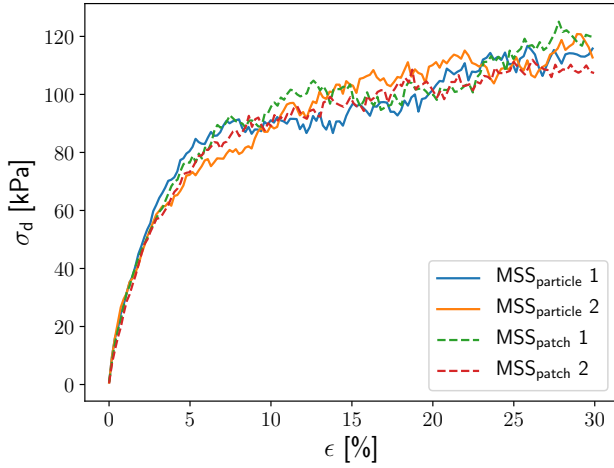
Table 2 Material parameters used in the simulation

	particles	membrane
radius / thickness [mm]	2.3 to 2.7	0.3
elastic modulus [Pa]	$4.6 \cdot 10^{10}$	$1.25 \cdot 10^6$
Poisson's ratio	0.245	1/3
friction coefficient	0.25	1.2

We consider two different systems: *case 1* – a cylinder of initial height 100 mm and radius 25 mm, and *case 2* – a cylinder of initial height 140 mm and radius



(a) Case 1. initial height 100 mm; radius 25 mm



(b) Case 2. initial height 140 mm; radius 35 mm

Fig. 5 Deviatoric stress against axial strain for two different geometries

35 mm. The numbers of particles used for the membrane and the granulate are given in Tab. 3.

Table 3 Number of granular and membrane particles in the simulations

	membrane particles		granular particles	
	case 1	case 2	case 1	case 2
MSS _{particle}	10440	20374	1690	4790
MSS _{patch}	1131	2214	1720	4670

Figure 5 shows the deviatoric stress, σ_d , as a function of the axial strain, ϵ . The different membrane representations, MSS_{particle} and MSS_{patch}, do not lead to significant differences of the stress-strain behavior.

Table 4 compares the computer time used to simulate a real time of 20 ms. The reduced number of par-

Table 4 Computer time used for different membrane representations. Real time is 20 ms

	case 1	case 2
MSS _{particle}	≈ 32 min	≈ 96 min
MSS _{patch}	≈ 5 min	≈ 17 min

ticles in MSS_{patch} accelerates the simulations by about the factor 5, compared to simulations using MSS_{particle}.

3.2 Friction test

A correct representation of frictional forces at contacts with the membrane is important for many applications. For instance, one of the mechanisms allowing a granular gripper to grasp an object relies on frictional forces [4]. By construction, an object gliding on a membrane modeled by particles cannot feel a constant (or, at least, smooth) force.

We demonstrate the smoothness of a membrane modeled by the here described model, and the resulting frictional forces by means of a simple sliding test: In MSS_{particle}, a membrane is modeled by vertex particles with spacing 1.33 mm. In MSS_{patch}, the membrane is modeled by patches of side length 1.33 mm.

For the test, we place a spherical particle of radius 2 mm on a membrane, the free motion of this particle is restricted to the vertical coordinate, perpendicular to the membrane. Its horizontal motion at constant velocity, 0.05 m/s, is enforced externally. Figure 6 shows the particle's vertical position and the frictional force in sliding direction.

For MSS_{particle} we see oscillations in both horizontal force and vertical position. For MSS_{patch}, we instead observe constant vertical position and constant friction force, as expected when a particle slides on an even plane.

4 Conclusions

Previous work using MSS for representing membranes within DEM simulations describe contacts between the granulate and confining membranes through contacts between the membrane's particles and the particles of the granulate. In this paper, we introduced a membrane model using surface patches. Contacts between granulate and the membrane are described by contacts between surface patches constituting the membrane and the particles of the granulate.

The model describes a closed surface by design, therefore, the number of particles in the MSS can

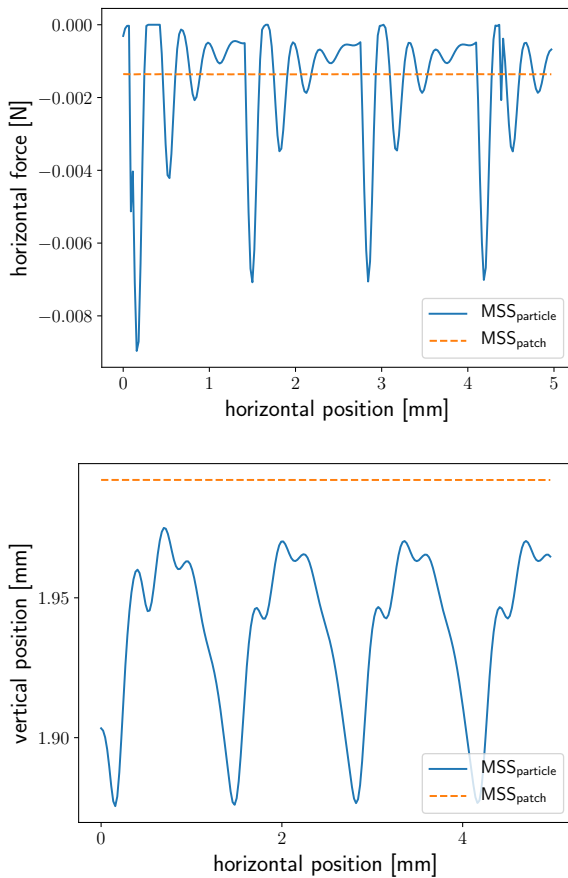


Fig. 6 The frictional force in horizontal direction felt a particle when moving on the surface of a membrane (upper image) and corresponding vertical position (lower image) vs the horizontal position for both considered membrane models. Rolling degree of freedom was suppressed

be reduced drastically. In a sample simulation modeling a triaxial test, we obtained an acceleration of the numerical method by about a factor five. The comparison of our results with the results using a traditional membrane description did not reveal significant differences in the physical behavior. We further demonstrated the new model's ability to represent smooth surfaces.

Acknowledgements We gratefully acknowledge funding by the Deutsche Forschungsgemeinschaft (DFG, German Research Foundation) – project number 411517575. The work was supported by the Interdisciplinary Center for Nanostructured Films (IZNF), the Competence Unit for Scientific Computing (CSC), and the Interdisciplinary Center for Functional Particle Systems (FPS) at Friedrich-Alexander Universität Erlangen-Nürnberg.

Conflict of interest

The authors declare that they have no conflict of interest.

References

1. Liu, A. J., Nagel, S. R.: Jamming is not just cool any more. *Nature* **396**, 21–22 (1998). DOI 10.1038/23819
2. O'Hern, C. S., Silbert, L. E., Liu, A. J., Nagel, S. R.: Jamming at zero temperature and zero applied stress: The epitome of disorder. *Phys. Rev. E* **68**, 011306 (2003). DOI 10.1103/PhysRevE.68.011306
3. Ciamarra, M. P., Nicodemi, M., Coniglio, A.: Recent results on the jamming phase diagram. *Soft Matter* **6**, 2871–2874 (2010). DOI 10.1039/B926810C
4. Brown, E., Rodenberg, N., Amend, J., Mozeika, A., Steltz, E., Zakin, M. R., Lipson, H., Jaeger, H. M.: Universal robotic gripper based on the jamming of granular material. *PNAS* **107**, 18809–18814 (2010). DOI 10.1073/pnas.1003250107
5. Hauser, S., Eckert, P., Tuleu, A., Ijspeert, A.: Friction and damping of a compliant foot based on granular jamming for legged robots. In: 2016 6th IEEE International Conference on Biomedical Robotics and Biomechatronics (BioRob), pp. 1160–1165 (2016). DOI 10.1109/BIOROB.2016.7523788
6. Fitzgerald, S. G., Delaney, G. W., Howard, D.: A Review of jamming actuation in soft robotics. *Actuators* **9**, 104 (2020). DOI 10.3390/act9040104
7. de Bono, J., McDowell, G., Wanatowski, D.: Discrete element modelling of a flexible membrane for triaxial testing of granular material at high pressures. *Geotech. Lett.* **2**, 199–203 (2012). DOI 10.1680/geolett.12.00040
8. Qu, T., Feng, Y. T., Wang, Y., Wang, M.: Discrete element modelling of flexible membrane boundaries for triaxial tests. *Comput. Geotech.* **115**, 103154 (2019). DOI 10.1016/j.compgeo.2019.103154
9. Wu, K., Sun, W., Liu, S., Zhang, X.: Study of shear behavior of granular materials by 3D DEM simulation of the triaxial test in the membrane boundary condition. *Adv. Powder Technol.* **32**, 1145–1156 (2021). DOI 10.1016/j.appt.2021.02.018
10. Götz, H., Santarossa, A., Sack, A., Pöschel, T., Müller, P.: Soft particles reinforce robotic grippers: Robotic grippers based on granular jamming of soft particles. *Granular Matter* **24**, 31 (2021). DOI 10.1007/s10035-021-01193-4
11. Götz, H., Pöschel, T.: Granular meta-material: Viscoelastic response of a bending beam. *Granular Matter* **sumitted** (2022)
12. Schäfer, J., Dippel, S., Wolf, D. E.: Force schemes in simulations of granular materials. *J. Phys. I France* **6**, 5–20 (1996). DOI 10.1051/jp1:1996129
13. Pöschel, T., Schwager, T.: *Computational Granular Dynamics: Models and Algorithms*. Springer-Verlag, Berlin ; New York (2005)
14. Kruggel-Emden, H., Simsek, E., Rickelt, S., Wirtz, S., Scherer, V.: Review and extension of normal force models for the Discrete Element Method. *Powder Technology* **171**, 157–173 (2007). DOI 10.1016/j.powtec.2006.10.004
15. Kruggel-Emden, H., Wirtz, S., Scherer, V.: A study on tangential force laws applicable to the discrete element

- method (DEM) for materials with viscoelastic or plastic behavior. *Chemical Engineering Science* **63**(6), 1523–1541 (2008). DOI 10.1016/j.ces.2007.11.025
16. Matuttis, H. G., Chen, J.: *Understanding the Discrete Element Method: Simulation of Non-Spherical Particles for Granular and Multi-body Systems*. Wiley (2014)
 17. Kot, M., Nagahashi, H.: Mass spring models with adjustable Poisson's ratio. *Vis. Comput.* **33**, 283–291 (2017). DOI 10.1007/s00371-015-1194-8
 18. Ostoja-Starzewski, M.: Lattice models in micromechanics. *Appl. Mech. Rev.* **55**, 35–60 (2002). DOI 10.1115/1.1432990
 19. Bridson, R., Marino, S., Fedkiw, R.: Simulation of clothing with folds and wrinkles. In: *Proceedings of the 2003 ACM SIGGRAPH/Eurographics Symposium on Computer Animation, SCA '03*, pp. 28–36. Eurographics Association, Goslar, DEU (2003)
 20. Hu, L., Hu, G. M., Fang, Z. Q., Zhang, Y.: A new algorithm for contact detection between spherical particle and triangulated mesh boundary in discrete element method simulations. *Int. J. Numer. Methods Eng.* **94**, 787–804 (2013). DOI 10.1002/nme.4487
 21. Weinhart, T., Orefice, L., Post, M., van Schrojenstein Lantman, M. P., Denissen, I. F. C., Tunuguntla, D. R., Tsang, J. M. F., Cheng, H., Shaheen, M. Y., Shi, H., Rapino, P., Grannonio, E., Losacco, N., Barbosa, J., Jing, L., Alvarez Naranjo, J. E., Roy, S., den Otter, W. K., Thornton, A. R.: Fast, flexible particle simulations — An introduction to MercuryDPM. *Comput. Phys. Commun.* **249**, 107129 (2020). DOI 10.1016/j.cpc.2019.107129
 22. Lubachevsky, B. D., Stillinger, F. H.: Geometric properties of random disk packings. *J. Stat. Phys.* **60**, 561–583 (1990). DOI 10.1007/BF01025983